bioRxiv preprint doi: https://doi.org/10.1101/151852; this version posted June 19, 2017. The copyright holder for this preprint (which was not certified by peer review) is the author/funder, who has granted bioRxiv a license to display the preprint in perpetuity. It is made available under aCC-BY-NC-ND 4.0 International license.

Cross-inhibition of JNK by p38 visualized by multiplexed fluorescence imaging.

Authors: Haruko Miura[1,3], Michiyuki Matsuda[1,2], Kazuhiro Aoki[3,4]*

Running Title: Live imaging of JNK and p38 activities

Affiliations:

[1]Laboratory of Bioimaging and Cell Signaling, Graduate School of Biostudies, Kyoto University, Sakyo-ku, Kyoto 606-8501, Japan.

[2]Department of Pathology and Biology of Diseases, Graduate School of Medicine, Kyoto University, Sakyo-ku, Kyoto 606-8501, Japan.

[3]Division of Quantitative Biology, Okazaki Institute for Integrative Bioscience, National Institute for Basic Biology, National Institutes of Natural Sciences, Okazaki, Aichi 444-8787, Japan.

[4]Department of Basic Biology, Faculty of Life Science, SOKENDAI (Graduate University for Advanced Studies), Myodaiji, Okazaki, Aichi 444-8787, Japan

*To whom correspondence should be addressed: k-aoki@nibb.ac.jp

Character count (no spaces): 24992

bioRxiv preprint doi: https://doi.org/10.1101/151852; this version posted June 19, 2017. The copyright holder for this preprint (which was not certified by peer review) is the author/funder, who has granted bioRxiv a license to display the preprint in perpetuity. It is made available under aCC-BY-NC-ND 4.0 International license.

Abstract

The stress activated protein kinases, Jun N-terminal kinase (JNK) and p38, orchestrate cellular responses to diverse environmental stresses and inflammatory signals. Crosstalk between JNK and p38 is emerging as an important regulatory mechanism in the inflammatory and stress responses. However, it is still unknown how this crosstalk regulates the signaling dynamics, cell-to-cell variabilities, and cell fate decisions at the single cell level. To address these issues, we established a multiplexed live-cell imaging system to simultaneously monitor JNK and p38 activities with high specificity and sensitivity at the single cell resolution. Exposure to various stresses and cytokines resulted in differential dynamics of JNK and p38 activation. In all cases, p38 negatively regulated JNK activity without affecting its own activation. We quantitatively demonstrate that p38 antagonizes JNK through both transcriptional and post-translational mechanisms with the relative contribution of the pathway depending on the stimulant. This cross-inhibition of JNK appears to generate cellular heterogeneity in JNK activity in response to inflammatory cytokines and stresses.

Keywords: crosstalk/fluorescence imaging/JNK/KTR/p38

bioRxiv preprint doi: https://doi.org/10.1101/151852; this version posted June 19, 2017. The copyright holder for this preprint (which was not certified by peer review) is the author/funder, who has granted bioRxiv a license to display the preprint in perpetuity. It is made available under aCC-BY-NC-ND 4.0 International license.

Introduction

The stress activated protein kinases (SAPKs), c-Jun N-terminal kinase (JNK) and p38, play important roles in the cellular response to a wide range of environmental stresses and inflammatory signals [1–3]. They are members of the mitogen-activated protein kinase (MAPK) family, which are activated in a three-tiered signaling cascade of sequentially activated protein kinases: MAPK kinase kinase (MAPKKK or MKKK), MAPK kinase (MAPKK or MKK), and MAPK. There are two MAPKKs that activate JNK, namely MKK4 and MKK7, while p38 is mainly activated by MKK3 and MKK6. In contrast to the limited number of MAPKKs, at least 15 MAPKKKs function upstream of p38 and/or JNK [4], allowing responses to diverse stress signals such as osmotic shock, oxidative stress, ultraviolet (UV) irradiation, heat shock, DNA damage, protein synthesis inhibitors, and pro-inflammatory cytokines. After activation, SAPKs phosphorylate their target substrates, including protein kinases, regulatory proteins, and various transcription factors, in order to exert their diverse functions [5,4].

Crosstalk between the JNK and p38 MAPK pathways has been described as an important regulatory mechanism in the context of both cell lines and animal models. In particular, increasing evidence supports that the p38 pathway can negatively regulate JNK, an example of so-called “cross-inhibition”. The first indication for this cross-inhibition is the finding that chemical inhibition and/or knockout (KO) of p38α increased JNK activity in response to pro-inflammatory cytokines and osmotic shock in a epithelial cell line, as well as in mouse embryonic fibroblasts (MEFs) and lipopolysaccharide (LPS)-stimulated macrophages [6]. As to the mechanism underlying this cross-inhibition, it has been proposed that p38 inhibits transforming growth factor-β-activated kinase (TAK1), a common upstream MAPKKK of p38 and JNK, by phosphorylation of TAK1 binding protein 1 (TAB1) [6]. In a study that further supported the idea of TAK1 as a mediator, tissue-specific loss of p38α was shown to result in aberrant activation of TAK1 and JNK in the intestine and skin after chemically induced inflammation, rendering the intestinal tissue more sensitive to inflammation-induced apoptosis [7]. Mice with liver-specific deletion of p38α exhibit increased hepatocyte proliferation in chemically induced liver cancer due to an increase in JNK activation, which in turn likely occurs via MKK7 [8]. These mice have also been shown to exhibit increased JNK and MKK3/6/4 activation after LPS injection [9]. Another

bioRxiv preprint doi: https://doi.org/10.1101/151852; this version posted June 19, 2017. The copyright holder for this preprint (which was not certified by peer review) is the author/funder, who has granted bioRxiv a license to display the preprint in perpetuity. It is made available under aCC-BY-NC-ND 4.0 International license.

study reported that activation of JNK by p38 inhibitors was dependent on the MAPKKK mixed-lineage protein kinase 3 (MLK3) and MKK4/MKK7 in a lung cancer cell line [10].

p38α is known to upregulate transcription of the dual-specificity protein phosphatase 1 (DUSP1), also known as MAPK phosphatase-1 (MKP-1), which dephosphorylates and inactivates p38 and JNK [11–14]. For example, myoblasts lacking p38α showed continuous proliferation under differentiation-promoting conditions, and this effect was caused by persistent JNK activation due to a reduction of DUSP1 [15]. Abrogation of p38α also led to greater JNK phosphorylation in macrophages and keratinocytes in response to LPS and UV irradiation through the reduced induction of DUSP1, respectively [16]. Moreover, DUSP1 depletion has been shown to increase JNK activity, and thereby sensitize MEFs to UV-induced apoptosis [17]. Taken together, these results demonstrate that p38α negatively regulates JNK signaling by different mechanisms, namely, post-translational modification at the level of an upstream MAPKKK and MAPKK and/or transcriptional induction of a JNK-inactivating phosphatase. Notably, these mechanisms are believed to be dependent on the cell type and stimulus [4]. Although the cross-inhibition of JNK by p38 and its physiological relevance have been well documented in cell populations by biochemical studies, the degree of cell-to-cell variability and the dynamics of crosstalk between JNK and p38 signaling at the single cell level have not been addressed due to the lack of suitable live cell imaging reporters.

Förster resonance energy transfer (FRET) biosensors are a powerful tool for monitoring kinase activity in living cells, and, indeed, FRET biosensors for JNK and p38 MAPK have already been developed [18–20]. However, simultaneous imaging of multiple kinase activities, which would be essential for crosstalk analysis in single cells, is technically very challenging with a FRET biosensor, since most FRET biosensors consist of YFP and CFP fluorescent proteins (FPs). Recently, Regot *et al.* developed kinase translocation reporter (KTR) technology, which allows multiplexed visualization of multiple kinase activities such as ERK, p38, and JNK in single cells [21]. These KTRs translate their kinase activity into a nucleocytoplasmic shuttling event, thus enabling the visualization of kinase activity with only one FP.

In this study, we present a multiplexed imaging system based on kinase

bioRxiv preprint doi: https://doi.org/10.1101/151852; this version posted June 19, 2017. The copyright holder for this preprint (which was not certified by peer review) is the author/funder, who has granted bioRxiv a license to display the preprint in perpetuity. It is made available under aCC-BY-NC-ND 4.0 International license.

translocation reporters for monitoring p38 and JNK activities with high specificity and sensitivity in single living cells. We then use this reporting system to measure p38 and JNK activity patterns in response to various stress stimuli, and quantitatively examine the mechanisms underlying the cross-inhibition of JNK by p38. Our data suggest that p38 negatively regulates JNK by post-translational and transcriptional mechanisms in a stimulus-specific manner, and that this cross-inhibition might be the origin of cell-to-cell variability in JNK activity.

Results and Discussion

Development of a multiplexed imaging system for p38 and JNK activities based on kinase translocation reporters

To visualize the activities of p38 and JNK simultaneously at the single cell resolution, we sought to implement a multiplexed imaging system based on genetically-encoded translocation reporters. This approach depends on the conversion of phosphorylation into a nucleocytoplasmic shuttling event. Such nucleocytoplasmic translocations have been described in some naturally occurring proteins [22–25], and more recently in the KTR technology [21]. Upon phosphorylation, the reporter is exported from the nucleus to the cytosol, and goes back to the nucleus upon dephosphorylation (Fig 1A). The kinase activity can be quantified by the ratio of the cytosolic to the nuclear fluorescence intensity (C/N ratio).

We attempted to apply the previously reported JNK and p38 KTRs to our study [21]. However, in our hands the prototype p38 KTR showed limited cytosolic translocation by anisomycin stress (Fig 1B), prompting us to develop an improved translocation-based reporter for p38 activity. Fortunately, it has been reported that the p38α substrate MK2 (MAPKAPK2) naturally shuttles between the nucleus and cytosol based on its phosphorylation status [26,27]. Earlier studies applied fluorescently tagged MK2 to screening of p38 inhibitors [28]. Therefore, we decided to use full-length MK2 as a quantitative live cell-imaging reporter for p38 activity. We found that mEGFP-MK2, which included the full length of MK2, outperformed p38 KTR in terms of the increased C/N ratio in response to anisomycin (Fig 1B). mEGFP-MK2 exhibited a greater anisomycin-stimulated fold increase in the C/N ratio (Fig 1EVA), indicating that

bioRxiv preprint doi: https://doi.org/10.1101/151852; this version posted June 19, 2017. The copyright holder for this preprint (which was not certified by peer review) is the author/funder, who has granted bioRxiv a license to display the preprint in perpetuity. It is made available under aCC-BY-NC-ND 4.0 International license.

the MK2-based reporter monitors p38 activity with higher sensitivity than the previously reported p38 KTR. To the best of our knowledge, this is the first study to characterize fluorescently tagged MK2 as a quantitative live cell imaging reporter for p38 activity.

For multiplexed imaging of JNK and p38 activities, we fused JNK KTR to mCherry and MK2 to monomeric Kusabira Orange (mKO). In addition, a near-infrared fluorescent protein (iRFP) flanked by nuclear localization signals (NLS) served as a nuclear marker (Fig 1C). The different fluorescent proteins in the red color range allow combination with FRET biosensors and blue light-induced optogenetics, if needed. To examine possible cross-excitation and/or bleed-through, we imaged HeLa cells expressing each reporter with all combinations of detection channels (Fig EV1B), and determined their relative contribution to the fluorescence. The bleed-through and cross-excitation of JNK KTR-mCherry, mKO-MK2, and NLS-iRFP-NLS were negligible under our imaging conditions, allowing multiplexed imaging of these reporters without linear unmixing.

For the following imaging experiments, we established HeLa cell lines stably-expressing each of the three reporters. The HeLa cell lines were established by transposon-mediated gene transfer, followed by drug selection and single cell cloning. To make the simultaneous expression in a different genetic background easier and faster, we also constructed a polycistronic vector, which we named pNJP (Nuclear, JNK, and p38 reporter). This vector consists of cDNAs of NLS-iRFP-NLS, JNK KTR-mCherry, and mKO-MK2, which are connected by self-cleaving P2A peptide sequences [29] (Fig EV1C). HeLa cells stably expressing NJP showed localizations of JNK KTR-mCherry, mKO-MK2, and NLS-iRFP-NLS that were comparable to those of the individually expressed reporters (Fig EV1D), indicating that the reporters were successfully separated from each other. This was further confirmed by western blot analysis (Fig EV1E). Of note, when JNK KTR-mCherry and mKO-MK2 were transiently overexpressed in HeLa cells, the increase in the C/N ratio upon saturated anisomycin stimulation (1.0 μg/ml) was negatively correlated with these expression levels (Fig EV1F), suggesting that the high expression level of the reporters may impede visualization of the translocation, probably due to the existence of a rate-limiting step in nuclear import/export. Meanwhile, in the range of stable expression, the

bioRxiv preprint doi: https://doi.org/10.1101/151852; this version posted June 19, 2017. The copyright holder for this preprint (which was not certified by peer review) is the author/funder, who has granted bioRxiv a license to display the preprint in perpetuity. It is made available under aCC-BY-NC-ND 4.0 International license.

C/N ratio was independent of the reporter expression levels (Fig EV1F).

JNK KTR-mCherry and mKO-MK2 monitor JNK and p38 activity, respectively, with high specificity and sensitivity

Next, we evaluated the dynamics and specificity of the reporters. For this purpose, we stimulated a clonal HeLa cell line stably expressing the three reporters, JNK KTR-mCherry, mKO-MK2, and NLS-iRFP-NLS, with 1.0 μg/ml anisomycin, a strong inducer of stress signaling pathways. Translocation of JNK KTR-mCherry and mKO-MK2 was readily observed (Fig 1D) and was quantified as the C/N ratio for single cells (Fig 1E). The mKO-MK2 and JNK KTR-mCherry C/N ratios started to increase approximately 5 and 10 min after stimulation, respectively. These C/N ratios reached maximal levels about 20 and 30 min after stimulation, respectively, and remained high thereafter (Fig 1E). Importantly, the anisomycin-stimulated increase in the C/N ratio of JNK KTR-mCherry could be specifically repressed by JNK inhibitor VIII, but not by the p38 inhibitor SB203580 (Fig 1F). In contrast, p38 inhibition increased the C/N ratio of JNK KTR-mCherry, as discussed in detail in a later section. As expected, the increase in the C/N ratio of mKO-MK2 was rapidly reduced by SB203580, but not by JNK inhibitor VIII (Fig 1F). Moreover, the anisomycin-induced increase in the C/N ratio of JNK KTR-mCherry was fully suppressed in *MAPK8* (*JNK1*) and *MAPK9* (*JNK2*) double KO cells, while translocation of mKO-MK2 was largely prevented in *MAPK14* (*p38α*) KO cells (Fig 1G). The KO of *JNK1/JNK2* and *p38α* was confirmed by western blotting (Fig EV1G). Taken together, these data demonstrate that JNK KTR-mCherry and mKO-MK2 specifically monitor JNK and p38α activities, respectively.

To further validate the dynamics of JNK KTR-mCherry and mKO-MK2, we compared the time courses of the C/N ratios to the endogenous phosphorylation of bulk JNK and p38 obtained by western blotting. The kinetics of the change in the JNK KTR-mCherry and mKO-MK2 C/N ratios upon stimulation with 1.0 μg/ml anisomycin were comparable to those of JNK and p38 phosphorylation, respectively, with a time lag of 5 to 10 min (Fig 1H and EV1H); the lag may have been attributable to the delayed substrate phosphorylation after kinase activation and/or nucleocytoplasmic shuttling.

To evaluate the sensitivity and dynamic range of JNK KTR-mCherry and mKO-MK2, we studied the anisomycin dose response. C/N ratios of mKO-MK2 and

bioRxiv preprint doi: https://doi.org/10.1101/151852; this version posted June 19, 2017. The copyright holder for this preprint (which was not certified by peer review) is the author/funder, who has granted bioRxiv a license to display the preprint in perpetuity. It is made available under aCC-BY-NC-ND 4.0 International license.

JNK KTR-mCherry showed modest switch-like responses as well as the endogenous phosphorylation of p38 and JNK (Fig 1I, EV1I and J); the EC50 values (sensitivities) were 8.2 ng/ml and 12.5 ng/ml, and the Hill coefficients were 2.3 and 2.8 for mKO-MK2 and JNK KTR-mCherry, respectively (Fig 1I). Plotting the C/N ratios against the levels of phosphorylated target kinase revealed a strong linear correlation, indicating that the dynamic range of the translocation reporters covers the full range of JNK and p38 activities upon anisomycin stimulation (Fig 1J). Taken together, the results showed that this system allows us to quantitatively monitor stress-induced p38 and JNK activity-dynamics with high specificity and sensitivity at the single cell level.

Crosstalk of JNK and p38 signaling

Prior work has provided compelling evidence of the interplay of p38 and JNK activities at a population level. Chemical inhibition or KO of *p38α* has led to JNK hyper-activation in several contexts, suggesting that p38 negatively regulates JNK [6–9,15–17,30]. Although this relationship has been well established in the cell population, it is virtually unknown how this crosstalk affects the dynamics and cell-to-cell variability of SAPK signaling at the single cell level. By using the aforementioned specific and sensitive imaging system for JNK and p38 activities, we investigated the crosstalk of JNK and p38 in individual cells. For this purpose, we stimulated the HeLa cells expressing the reporter system with pro-inflammatory cytokines (10 ng/ml TNFα, 10 ng/ml IL-1β) or stress inputs (10 ng/ml anisomycin, 200 mM sorbitol, and 100 J/m^2 UV-C) in the presence or absence of p38 inhibitors and measured the JNK and p38 activities (Fig 2A-C). In control cells, we observed distinct kinetics of JNK and p38 activities for the different stimuli; TNFα and IL-1β stimulation resulted in transient JNK and p38 activation, while the other stress inputs induced JNK and p38 activities in a sustained fashion within the time frame of observation (Fig 2B-C). At the single cell level, we found that the JNK activity varied among individual cells, while the p38 response was more homogenous for all stimulants (Fig 2A). When cells were pretreated with two different p38 inhibitors, SB203580 and VX-745, JNK activity was significantly increased under each inflammatory and stress condition, and its cellular heterogeneity seemed to be reduced (Fig 2A-C). We observed a linear negative correlation of anisomycin-induced JNK and p38 activities across p38 inhibitor concentrations (Fig 2D

bioRxiv preprint doi: https://doi.org/10.1101/151852; this version posted June 19, 2017. The copyright holder for this preprint (which was not certified by peer review) is the author/funder, who has granted bioRxiv a license to display the preprint in perpetuity. It is made available under aCC-BY-NC-ND 4.0 International license.

and EV2A). We also tested the effect of JNK inhibition on p38 activity. Surprisingly, JNK inhibitor VIII reduced p38 activity in response to 10 ng/ml TNFα, 10 ng/ml IL-1β, 10 ng/ml anisomycin, and 100 J/m^2 UV-C (Fig EV2B). This might indicate that JNK signaling positively regulates p38 activity, but we could not exclude the possibility of off-target effects of JNK inhibitor VIII. We therefore focused on the effect of p38 signaling on JNK activity in the present study.

To test how cross-inhibition of JNK by p38 desensitizes JNK activation upon anisomycin treatment, we examined the dose-dependency of JNK activities in control and SB203580-pretreated cells. SB203580 shifted the EC50 of the JNK response to lower concentration and converted the JNK activity response to a more switch-like output (Fig 2E). At the single cell level, JNK did not show an "all-or-none" response, but rather a graded response, as evidenced by the unimodal distribution of JNK activity (Fig 2F). This was especially evident for stimulation at around the EC50 concentration (7.5 ng/ml for SB203580 pretreatment), which yielded in only one peak of half maximal JNK activities (Fig 2F). Although bi-stability has been reported for individual anisomycin-stressed HeLa cells using a FRET biosensor [18], meaning that cells either show a full or no response, our data suggest that the JNK activation in the same system at the single cell level was graded. This difference may have been due to the higher sensitivity of JNK KTR-mCherry to lower anisomycin concentrations (around 10 ng/ml), at which the FRET biosensor failed to detect JNK activity [18]. To confirm the cross-inhibition of JNK by p38 at the endogenous level, we analyzed the endogenous activation of JNK after 1 h of stress exposure by western blotting. Consistent with the imaging data, SB203580 pretreatment resulted in significantly higher JNK phosphorylation than the DMSO control under all the stress conditions examined (Fig 2G). Interestingly, in the same samples SB203580 did not affect phosphorylation of p38 itself, implying that p38 does not induce negative feedback in the observed timescale of 1 h, but rather specifically cross-inhibits JNK activity (Fig 2G).

Post-translational and transcriptional mechanisms contribute to cross-inhibition of JNK by p38

We next examined what kind of mechanisms mediated the negative regulation of JNK by p38. Previous studies have demonstrated two main possible mechanisms: Post-

bioRxiv preprint doi: https://doi.org/10.1101/151852; this version posted June 19, 2017. The copyright holder for this preprint (which was not certified by peer review) is the author/funder, who has granted bioRxiv a license to display the preprint in perpetuity. It is made available under aCC-BY-NC-ND 4.0 International license.

translational regulation of an upstream MAPKK/MAPKKK or transcriptional induction of a phosphatase such as DUSP1. It is suggested that the mechanism underlying the cross-inhibition of JNK by p38 depends on the cell type and stimulus [4,31].

To dissect the post-translational and transcriptional mechanisms, we pretreated cells with an inhibitor of transcription actinomycin D or SB203580, followed by exposure of each stress input for a longer duration (2 h) in order to clearly observe the transcriptional regulation. Interestingly, actinomycin D had different effects according to the stimulant. Actinomycin D potentiated the stimulation of JNK activity by IL-1β, anisomycin, or UV-C, while the actinomycin D treatment has almost no effect on the TNFα- and sorbitol-induced JNK activities (Fig 3A and EV3). In general, p38 inhibition resulted in higher JNK activities than actinomycin D treatment alone (Fig 3A and EV3). It should be noted that we used anisomycin below the IC50 of protein synthesis [32], so that potentially induced phosphatase transcripts could be translated. With regard to p38 activities, actinomycin D counteracted the downregulation of IL-1β- and TNFα-stimulated p38 activities, but had no substantial effect on the sustained anisomycin, sorbitol, and UV-C-induced p38 activities (Fig 3A and EV3), indicating that phosphatases induced by these stress stimuli did not inhibit p38 and rather specifically inactivated JNK. The difference of JNK activity between the p38 inhibitor and actinomycin D indicated the effect of a post-translational mechanism on the cross-inhibition of JNK by p38, enabling us to roughly quantify how much these two pathways contribute to the cross-inhibition of JNK by p38 under various stress and inflammatory conditions (Fig 3B). We found that, in response to TNFα and osmotic shock, cross-inhibition is mainly mediated by post-translational mechanisms, while in the case of IL-1β, anisomycin, and UV-C stress, both modes of cross-inhibition seem to operate (Fig 3B). Since it has been reported that p38 can induce DUSP1 gene expression in response to pro-inflammatory cytokines and various stresses [16,17,20,33], it is likely that DUSP1 was involved in the transcriptional cross-inhibition of JNK. However, it is unclear why DUSP1, a phosphatase of JNK and p38, would not inactivate p38 in our system, when exposed to anisomycin and UV-C.

To explore whether the contribution of the two modes of cross-inhibition could be influenced by the stimulation strength, we examined the JNK activities in the control, actinomycin D-pretreated and SB203580-pretreated cells after stimulation with

bioRxiv preprint doi: https://doi.org/10.1101/151852; this version posted June 19, 2017. The copyright holder for this preprint (which was not certified by peer review) is the author/funder, who has granted bioRxiv a license to display the preprint in perpetuity. It is made available under aCC-BY-NC-ND 4.0 International license.

various doses of IL-1β, as IL-1β made equal contributions to the post-translational and transcriptional cross-inhibition in the earlier experiments. Indeed, actinomycin D affected the graded JNK response upon IL-1β stimulation starting at a higher concentration (EC50 ~ 1.5 ng/ml) than SB203580 (EC50 ~ 0.6 ng/ml), suggesting that post-translational cross-inhibition was more sensitive to the IL-1β dose than transcriptional cross-inhibition (Fig 3C).

Phosphorylation of TAB1 downregulates cytokine-induced JNK, but not p38 activity

Next, we further investigated the mechanisms underlying post-translational cross-inhibition. To examine whether TAB1 and TAK1 were involved in the regulation of JNK by p38, we first assessed whether JNK and p38 activities were dependent on TAB1 and TAK1 under each condition by using CRISPR/Cas9-mediated KO cells (Fig EV4A, B). We found that the TNFα- and IL-1β-induced JNK activities were almost completely and sorbitol-induced JNK activities partially suppressed in *TAB1* and *MAP3K7* (*TAK1*) KO cells, while anisomycin and UV-C induced JNK activities were not decreased by *TAB1* KO (Fig. 4A). On the other hand, TNFα treatment showed a strong dependency of p38 activation on only TAK1, but surprisingly not TAB1 (Fig 4B). IL-1β-induced p38 activation was partially suppressed in *TAK1* KO and *TAB1* KO cells (Fig 4B). Under the other stress conditions, *TAB1* and *TAK1* KO had only slight or no effect on p38 activation (Fig 4B). Thus, cytokine stimulations, i.e., TNFα and IL-1β stimulations, and osmotic shock appeared to employ the TAK1/TAB1 complex for JNK activation.

The phosphorylation of TAB1 by p38 has been reported to be involved in JNK cross-inhibition upon TNFα and IL-1β stimulation [6]. Therefore, we mutated the p38 phosphorylation sites in TAB1, namely Ser423 and Thr431, to alanine (SATA), and examined whether expression of the TAK1 SATA mutant rescued the cross-inhibition of JNK by p38 in *TAB1* KO HeLa cells. As we expected, the TAB1 wildtype could rescue the cross-inhibition of JNK, whereas TAB1 SATA caused significantly higher JNK activities than did the TAB1 wildtype in response to TNFα, IL-1β, and sorbitol (Fig. 4C). In contrast, p38 activity seemed not to be affected by the SATA mutation (Fig 4C). Although we speculated that the phosphorylation of TAB1 by p38 might affect the binding to TAK1, TAB1 SATA mutation had no obvious consequence on the binding of TAB1 to TAK1 as analyzed by co-immunoprecipitation (Fig EV4C). These results

bioRxiv preprint doi: https://doi.org/10.1101/151852; this version posted June 19, 2017. The copyright holder for this preprint (which was not certified by peer review) is the author/funder, who has granted bioRxiv a license to display the preprint in perpetuity. It is made available under aCC-BY-NC-ND 4.0 International license.

support those of the previous study showing that p38 inhibition or KO increased LPS, TNFα, IL-1β, and sorbitol induced TAK1 activity and JNK phosphorylation. Along with the finding that p38 inhibition had no significant effect on the phosphorylation of p38 itself after 1 h of treatment with various stimuli (Fig 2G), our observations based on kinase activity reporters and rescue of *TAB1* KO cells strongly suggested that phosphorylation of TAB1 on Ser423 and Thr431 reduces TAK1 activity for JNK activation, but probably not p38 activation in living cells. This could be explained by the result that cytokine-induced p38 activities were less dependent on TAB1 than JNK activities. Collectively, these data indicate that TAB1 phosphorylation by p38 contributes to cross-inhibition of JNK in response to pro-inflammatory cytokines, but not to negative feedback control of p38 (Fig 4D).

Cross-inhibition of JNK by p38 induces heterogeneity of JNK signaling among cells

Finally, we explored the role of cross-inhibition of JNK. As mentioned earlier, JNK activity varied among single cells after cytokine and stress exposure, while p38 activity was more homogeneous in the same cells (Fig 2A, C, Movie EV1). Closer analysis revealed that the distribution of kinase activity after 1 h of incubation under anisomycin stress (10 ng/ml) was broader for JNK, with a coefficient of variation (CV) of ~ 0.39, than for p38, with a CV of ~ 0.21 (Fig 5A). Remarkably, inhibition of p38 not only shifted the distribution of JNK activities to higher levels (Fig 5A), but also reduced the variation of JNK activity to a CV of ~ 0.18, which is approximately half the value of the control (Fig 5A). This effect was also well represented in the time evolution of the CV upon stress stimulation; anisomycin treatment gradually increased the CV of JNK activity, while inhibition of p38 by SB203580 reduced the CV of JNK activity after anisomycin stimulation (Fig 5B). Of note, the CV values reached the minimum 30 min after anisomycin treatment, even though the JNK activity had not yet reached its maximal level at that time (Fig 2B). This result implies that the saturation of JNK activity via the suppression of cross-inhibition does not necessarily contribute to the decrease in heterogeneity of JNK activity. In the case of p38 activity, the CV remained constant over the time course of anisomycin stimulation (Fig 5B). This trend was valid for other stimuli as well. SB203580 led to smaller CVs in JNK activity in response to 10 ng/ml TNFα, 10 ng/ml IL-1β, 200 mM sorbitol, and 100 J/m^2 UV-C, in comparison

bioRxiv preprint doi: https://doi.org/10.1101/151852; this version posted June 19, 2017. The copyright holder for this preprint (which was not certified by peer review) is the author/funder, who has granted bioRxiv a license to display the preprint in perpetuity. It is made available under aCC-BY-NC-ND 4.0 International license.

to the control (Fig 5C and EV5). These results indicate that inflammatory cytokines and stresses cause the increase in heterogeneity in JNK activity among individual cells through the cross-inhibition by p38, which shows more uniform activation.

In summary, the establishment of a specific and sensitive imaging system for JNK and p38 allowed us to determine that p38 antagonizes JNK under diverse stress conditions by both post-translational and transcriptional mechanisms. The relative contribution of each mode of regulation depends on the stimulus. Cross-inhibition of JNK upon TNFα and sorbitol treatment was largely dependent on post-translational mechanisms, while the downregulations of JNK activity upon IL-1β, anisomycin, and UV-C stress were post-translationally and transcriptionally mediated. In all the stress stimuli tested in this study, cross-inhibition of JNK by p38 resulted in an increase in heterogeneous JNK activity among single cells (Fig 5D), suggesting that this is a common mechanism underlying JNK and p38 signaling. It would be interesting to study whether this heterogeneity in JNK activity translates to a heterogeneous phenotypic response, such as transcription of pro-inflammatory genes or apoptosis, or whether the phenotype is robust to the cell-to-cell variability of JNK signaling. Indeed, intrinsic noise of gene expression results in an increase in cellular heterogeneity that is known as non-genetic heterogeneity, and eventually leads to resistance or persistence to anticancer drugs or antibiotics at the population level [34,35]. According to this mechanism, it is plausible that the heterogeneity of JNK activity generated by cross-inhibition from p38 confers resistance to cells against stress stimuli. Future studies will be needed to unveil how cross-inhibition by p38 leads to cellular heterogeneity of JNK activity. Our highly specific and sensitive multiplexed imaging system will be useful to quantitatively evaluate the interplay of p38 and JNK, revealing the heterogeneity of their interaction among single cells, and ultimately the role of their activity dynamics in phenotypic outcomes in response to stress and inflammatory signals.

bioRxiv preprint doi: https://doi.org/10.1101/151852; this version posted June 19, 2017. The copyright holder for this preprint (which was not certified by peer review) is the author/funder, who has granted bioRxiv a license to display the preprint in perpetuity. It is made available under aCC-BY-NC-ND 4.0 International license.

Materials and Methods

Plasmids

Plasmids were constructed by standard molecular biology methods. The nuclear localization signal (NLS) of SV40 large T antigen (PKKKRKV) was added to the N- and C-termini of iRFP by PCR and the construct was cloned into the pT2Apuro vector [36], a Tol2 transposon vector with IRES-*pac* (puromycin resistance gene), generating pT2Apuro-NLS-iRFP-NLS. The pT2A vector was a kind gift from Dr. K. Kawakami (National Institute for Genetics, Japan). JNK KTR was amplified by PCR from pLentiPGK Puro DEST JNKKTRClover [21], which was a kind gift from Dr. M. Covert (Addgene plasmid #59151), and cloned into the eukaryotic expression vector pCAGGS [37] or pPBbsr, a piggyBac transposon vector with IRES-*bsr* (blasticidin S resistance gene) [38], along with mCherry, resulting in pCAGGS-JNK KTR-mCherry and pPBbsr-JNK KTR-mCherry. The pPB backbone was a kind gift from Dr. A. Bradley (Wellcome Trust Sanger Institute, UK). p38 KTR [21] was synthesized by PCR from annealed sense- and antisense oligonucleotides and cloned into a pPBbsr-mEGFP vector to generate pPBbsr-p38 KTR-mEGFP. For pCAGGS-mKO-MK2, pPBbsr-mKO-MK2, and pPBbsr-mEGFP-MK2, the cDNA of human MAPKAPK2 (MK2) was amplified by PCR from a HeLa cDNA library and inserted into the pCAGGS or pPBbsr backbone together with mEGFP or mKO. To construct a polycistronic vector encoding NLS-iRFP-NLS, JNK KTR-mCherry, and mKO-MK2, sequences for the self-cleaving P2A peptide (GSGATNFSLLKQAGDVEENPGP) were PCR-cloned between the reporters, and the polycistronic cassette was inserted into the pPBbsr backbone to generate pNJP. The cDNAs of human TAB1 and TAK1 were obtained from HeLa cDNA by PCR, and S423A T431A / S423E T431E point mutations were introduced into TAB1 by two-step overlap-extension PCR. The cDNAs of TAB1-wt, SATA, SETE, and TAK1 were subcloned into pCSIIneo, a lentivirus vector with IRES-*neo* (neomycin resistance gene), pCAGGS-Flag, or pCAGGS-mEGFP vectors to generate pCSIIneo-TAB1-wt, pCSIIneo-TAB1-SATA, pCAGGS-Flag-TAB1-wt, pCAGGS-Flag-TAB1-SATA, pCAGGS-Flag-TAB1-SETE, and pCAGGS-mEGFP-TAK1. The lentiviral CSII-EF backbone vector was a kind gift from Dr. H. Miyoshi (RIKEN, Japan). lentiCRISPR v2 was a kind gift from Dr. F. Zhang (Addgene plasmid #52961) [39].

bioRxiv preprint doi: https://doi.org/10.1101/151852; this version posted June 19, 2017. The copyright holder for this preprint (which was not certified by peer review) is the author/funder, who has granted bioRxiv a license to display the preprint in perpetuity. It is made available under aCC-BY-NC-ND 4.0 International license.

Reagents

Anisomycin and actinomycin D were purchased from Sigma Aldrich, JNK inhibitor VIII from Calbiochem, SB203580 from Selleck Chemicals, and VX-745 from AdipoGen. Sorbitol was from Wako. Recombinant human TNFα and recombinant human IL-1β were acquired from R&D Systems. Blasticidin S, puromycin, and G418 were purchased from InvivoGen. The primary antibodies against p38 (#9212), phospho-p38 (Thr180/Tyr182) (#9216), JNK (#9252), phospho-JNK (Thr183/Tyr185) (#9355), JNK1 (#3708), JNK2 (#9258), TAK1 (#5206) and TAB1 (#3226) were purchased from Cell Signaling Technology. Anti-α-tubulin (CP06) was obtained from Calbiochem. Anti-Flag M5 antibody (F4042) was purchased from Sigma Aldrich. Anti-mCherry (ab167453) and anti-monomeric Kusabira Orange 2 (PM051M) antibodies were obtained from Abcam and MBL, respectively. Anti-GFP serum was prepared in our laboratory. Secondary antibodies IRDye 680LT goat anti-rabbit IgG and IRDye 800CW donkey anti-mouse IgG were purchased from LI-COR Biosciences. Irradiation with a defined dose of 100 J/m^2 UV-C light (254 nm) was performed using a CL-100 Ultraviolet Crosslinker (UVP).

Cell culture and cell line generation

HeLa cells were purchased from the Human Science Research Resources Bank (Japan) and were maintained in Dulbecco's Modified Eagle's Medium (DMEM) high glucose (Wako; Nacalai) supplemented with 10% fetal bovine serum (Sigma Aldrich). Antibiotics were added, when applicable. For transient expression, pCAGGS vectors were transfected using 293fectin (Invitrogen) according to the manufacturer's instructions. To establish stable cell lines expressing the fluorescent reporters, PiggyBac- and Tol2 transposon-based systems were applied. The reporters encoding pPBbsr or pT2Apuro vectors were co-transfected with the transposase encoding pCMV-mPBase (neo-) vector (a kind gift of Dr. A. Bradley, Wellcome Trust Sanger Institute, UK) and pCAGGS-T2TP vector (a kind gift of Dr. K. Kawakami, National Institute for Genetics, Japan), respectively, using 293fectin. One day after transfection, cells were selected with 20 μg/ml blasticidin S or 1 μg/ml puromycin for at least one week. To obtain the triple reporter cell line expressing NLS-iRFP-NLS, JNK KTR-mCherry, and mKO-MK2 simultaneously, the reporters were introduced based on the PiggyBac and

bioRxiv preprint doi: https://doi.org/10.1101/151852; this version posted June 19, 2017. The copyright holder for this preprint (which was not certified by peer review) is the author/funder, who has granted bioRxiv a license to display the preprint in perpetuity. It is made available under aCC-BY-NC-ND 4.0 International license.

Tol2 transposon system, and single cells were cloned and screened for iRFP, mCherry, and mKO expression. For easier generation of KO cell lines expressing the three reporters, the polycistronic vector pNJP was stably transfected using the PiggyBac transposon system. However, the expression levels of the polycistronic construct were reduced compared to the individually expressed reporters (Fig EV1E). To complement *TAB1* KO cells with the wildtype or mutant TAB1, lentivirus-mediated gene transfer was used. In brief, the lentiviral pCSIIneo vector was transfected into Lenti-X 293T cells (Clontech) together with the packaging plasmid psPAX2, which was a gift from Dr. D. Trono (Addgene plasmid #12260), and pCMV-VSV-G-RSV-Rev (a kind gift of Dr. Miyoshi, RIKEN, Japan) by using the linear polyethyleneimine "Max" MW 40,000 (Polyscience). After two days, target cells were infected with the virus-containing media. Beginning at two days after infection, the cells were selected by at least one week of treatment with 1 mg/ml G418. All cells were maintained in a humidified atmosphere of 5% CO_2 at 37 ˚C.

CRISPR/Cas9 mediated KO

For CRISPR/Cas9-mediated KO of human *MAPK14*, *MAPK8*, *MAPK9*, *MAP3K7*, and *TAB1* genes, single guide RNAs (sgRNA) targeting the first exon were designed using the CRISPR Design online tool (http://crispr.mit.edu, Zhang Lab, MIT). The following targeting sequences were used: *MAPK14*, AGCTCCTGCCGGTAGAACGT; *MAPK8*, ACGCTTGCTTCTGCTCATGA; *MAPK9*, TCAGTTTTATAGTGTGCAAG; *TAB1*, CCTCCTCTGCGCCGCCATCT; *MAP3K7*, CATCTCACCGGCCGAAGACG. Annealed Oligo DNAs for the sgRNAs were cloned into the lentiCRISPR v2 vector (Addgene plasmid #52961) [39] and the sgRNA/Cas9 cassettes were introduced into HeLa cells by lentiviral gene transfer. Infected cells were selected using 2 μg/ml puromycin and single cells were cloned.

Western blotting

HeLa cells were lysed in 1x SDS sample buffer (62.5 mM Tris-HCl pH 6.8, 12% glycerol, 2% SDS, 0.004% Bromo Phenol Blue, and 5% 2-mercaptoethanol). After sonication, the samples were separated by SDS-polyacrylamide gel electrophoresis and transferred to polyvinylidene membranes (Millipore). After blocking with Odyssey

bioRxiv preprint doi: https://doi.org/10.1101/151852; this version posted June 19, 2017. The copyright holder for this preprint (which was not certified by peer review) is the author/funder, who has granted bioRxiv a license to display the preprint in perpetuity. It is made available under aCC-BY-NC-ND 4.0 International license.

blocking buffer (LI-COR) or skim milk for 1 h, the membranes were incubated with primary antibodies diluted in Odyssey blocking buffer or TBS Tween20 overnight, followed by secondary antibodies diluted in Odyssey blocking buffer. Fluorescent signals were detected by an Odyssey Infrared scanner (LI-COR) and analyzed by the Odyssey imaging software.

Co-Immunoprecipitation

HeLa cells were co-transfected with pCAGGS-mEGFP-TAK1 and either pCAGGS-TAB1-wt, SATA, or SETE using 293fectin according to the manufacturer's instructions. One day after transfection, cells were lysed in 1% Triton-X lysis buffer and spun down to remove cell debris. Anti-GFP serum coupled to Protein A Sepharose Fast Flow matrix (GE Healthcare) was used to immune-precipitate mEGFP-TAK1 from the lysate for 2 h at 4ºC under rotation. The beads were washed three times in lysis buffer and then boiled in 1x SDS sample buffer at 95C. The supernatant was subjected to SDS-PAGE and Western blot analysis.

Live cell imaging

HeLa cells stably expressing the fluorescent reporters were grown on 35 mm glass-bottom dishes (Asahi Techno Glass) or four-compartment 35 mm glass-bottom dishes (Greiner Bio-One) for at least 24 h and starved in FluoroBrite DMEM (Life Technologies) supplemented with 1x GlutaMax (Life Technologies) and 0.2% fetal bovine serum for about 3 h. When applicable, cells were pretreated with inhibitors about 15 min before imaging and treated with stimulants. Images were acquired on an IX81 inverted microscope (Olympus), which was equipped with a Retiga 4000R cooled Mono CCD camera (QImaging), a Spectra-X light engine illumination system (Lumencor), an IX2-ZDC laser-based autofocusing system (Olympus), a UPlanSApo 60x/1.35 oil objective lens (Olympus), a UPlanSApo 20x/0.75 dry objective lens (Olympus), a MAC5000 controller for filter wheels and XY stage (Ludl Electronic Products), an incubation chamber (Tokai Hit), and a GM-4000 CO_2 supplier (Tokai Hit). The following filters and dichroic mirrors were used: for iRFP, a FF408/504/581/667/762 dichroic mirror (Semrock), and a 700/longpass emission filter (Semrock); for mCherry, a 580/20 excitation filter (Semrock), a 20/80 beamsplitter

bioRxiv preprint doi: https://doi.org/10.1101/151852; this version posted June 19, 2017. The copyright holder for this preprint (which was not certified by peer review) is the author/funder, who has granted bioRxiv a license to display the preprint in perpetuity. It is made available under aCC-BY-NC-ND 4.0 International license.

dichroic mirror (Chroma), and an FF01-641/75 emission filter (Semrock); for mKO, a 543/3 excitation filter (Semrock), a 20/80 beamsplitter dichroic mirror (Chroma), and a 563/9 emission filter (Semrock). The microscope was controlled by MetaMorph software (Molecular Devices).

Image analysis

Images were processed using the MetaMorph software as previously described [40]. For multiplexed imaging of translocation reporters, the background was corrected by subtraction of blank positions (medium only) or minimum planes to flat-field the images. Regions of interest were set in the nucleus and cytosol of single cells and the average value of their fluorescence intensities was measured. The ratio of the cytosolic and nuclear intensity (C/N ratio) was calculated using Excel software (Microsoft Corporation).

Numerical analysis

For non-linear regression of dose responses, we utilized solver functions in Microsoft Excel and fitted the experimental data with the Hill function to obtain EC50 and nH values.

Statistical analysis

Statistical analysis was conducted using Microsoft Excel software. For comparison of two datasets, a two tailed, unpaired Student's *t*-test was performed according to the result of the F-test. P values < 0.05 were considered significant at the following levels: $*p<0.05$, $**p< 0.01$, $***p<0.001$.

bioRxiv preprint doi: https://doi.org/10.1101/151852; this version posted June 19, 2017. The copyright holder for this preprint (which was not certified by peer review) is the author/funder, who has granted bioRxiv a license to display the preprint in perpetuity. It is made available under aCC-BY-NC-ND 4.0 International license.

Acknowledgements

We thank Dr. A. Bradley (pPB, pCMV-mPBase), Dr. M. Covert (pLentiPGK Puro DEST JNKKTRClover), Dr. K. Kawakami (pT2A, pCAGGS-T2TP), Dr. H. Miyoshi (CSII-EF, pCMV-VSV-G-RSV-Rev), Dr. D. Trono (psPAX2), and Dr. F. Zhang (lentiCRISPR v2) for providing plasmids. We are grateful to the members of the Matsuda Laboratory and Aoki Laboratory for their helpful discussions. A. Kawagishi, K. Hirano, and N. Nishimoto are also to be thanked for their technical assistance. K.A. and M.M. were supported by the Platform for Dynamic Approaches to Living Systems from the Ministry of Education, Culture, Sports, and Science, Japan, and CREST, JST. K.A. was supported by JSPS KAKENHI Grants (no. 16H01425, 16H01447, 16KT0069) and by a Takeda Science Foundation. H.M. was supported by a Grant-in-Aid for JSPS Fellows from MEXT, Japan.

Author contributions

H.M. and K.A. designed the research; H.M. performed the experiments and analyzed the data. H.M., K.A. and M.M. wrote the paper.

Conflict of interest

The authors declare that they have no conflict of interest.

bioRxiv preprint doi: https://doi.org/10.1101/151852; this version posted June 19, 2017. The copyright holder for this preprint (which was not certified by peer review) is the author/funder, who has granted bioRxiv a license to display the preprint in perpetuity. It is made available under aCC-BY-NC-ND 4.0 International license.

References

1. Johnson GL, Lapadat R (2002) Mitogen-Activated Protein Kinase Pathways Mediated by ERK, JNK, and p38 Protein Kinases The Protein Kinase Complement of the Human Genome. *Science* **298**: 1911–1912.

2. Cuadrado A, Nebreda AR (2010) Mechanisms and functions of p38 MAPK signalling. *Biochem J* **429**: 403–417.

3. Weston CR, Davis RJ (2007) The JNK signal transduction pathway. *Curr Opin Cell Biol* **19**: 142–149.

4. Wagner EF, Nebreda ÁR (2009) Signal integration by JNK and p38 MAPK pathways in cancer development. *Nat Rev Cancer* **9**: 537–549.

5. Raman M, Chen W, Cobb MH (2007) Differential regulation and properties of MAPKs. *Oncogene* **26**: 3100–3112.

6. Cheung PCF, Campbell DG, Nebreda AR, Cohen P (2003) Feedback control of the protein kinase TAK1 by SAPK2a/p38alpha. *EMBO J* **22**: 5793–5805.

7. Caballero-Franco C, Choo M-K, Sano Y, Ritprajak P, Sakurai H, Otsu K, Mizoguchi A, Park JM (2013) Tuning of protein kinase circuitry by p38α is vital for epithelial tissue homeostasis. *J Biol Chem* **288**: 23788–23797.

8. Hui L, Bakiri L, Mairhorfer A, Schweifer N, Haslinger C, Kenner L, Komnenovic V, Scheuch H, Beug H, Wagner EF (2007) p38alpha suppresses normal and cancer cell proliferation by antagonizing the JNK-c-Jun pathway. *Nat Genet* **39**: 741–749.

9. Heinrichsdorff J, Luedde T, Perdiguero E, Nebreda AR, Pasparakis M (2008) p38 alpha MAPK inhibits JNK activation and collaborates with IkappaB kinase 2 to

bioRxiv preprint doi: https://doi.org/10.1101/151852; this version posted June 19, 2017. The copyright holder for this preprint (which was not certified by peer review) is the author/funder, who has granted bioRxiv a license to display the preprint in perpetuity. It is made available under aCC-BY-NC-ND 4.0 International license.

prevent endotoxin-induced liver failure. *EMBO Rep* **9**: 1048–1054.

10. Muniyappa H, Das KC (2008) Activation of c-Jun N-terminal kinase (JNK) by widely used specific p38 MAPK inhibitors SB202190 and SB203580: A MLK-3-MKK7-dependent mechanism. *Cell Signal* **20**: 675–683.

11. Chi H, Barry SP, Roth RJ, Wu JJ, Jones EA, Bennett AM, Flavell RA (2006) Dynamic regulation of pro- and anti-inflammatory cytokines by MAPK phosphatase 1 (MKP-1) in innate immune responses. *Proc Natl Acad Sci U S A* **103**: 2274–2279.

12. Zhao Q, Wang X, Nelin LD, Yao Y, Matta R, Manson ME, Baliga RS, Meng X, Smith C V, Bauer JA, et al. (2005) MAP kinase phosphatase 1 controls innate immune responses and suppresses endotoxic shock. *J Exp Med* **203**: jem.20051794.

13. Hammer M, Mages J, Dietrich H, Servatius A, Howells N, Cato ACB, Lang R (2006) Dual specificity phosphatase 1 (DUSP1) regulates a subset of LPS-induced genes and protects mice from lethal endotoxin shock. *J Exp Med* **203**: 15–20.

14. Ananieva O, Darragh J, Johansen C, Carr JM, McIlrath J, Park JM, Wingate A, Monk CE, Toth R, Santos SG, et al. (2008) The kinases MSK1 and MSK2 act as negative regulators of Toll-like receptor signaling. *Nat Immunol* **9**: 1028–1036.

15. Perdiguero E, Ruiz-Bonilla V, Gresh L, Hui L, Ballestar E, Sousa-Victor P, Baeza-Raja B, Jardi M, Bosch-Comas A, Esteller M, et al. (2007) Genetic analysis of p38 MAP kinases in myogenesis: fundamental role of p38alpha in abrogating myoblast proliferation. *Embo J* **26**: 1245–1256.

16. Kim C, Sano Y, Todorova K, Carlson BA, Arpa L, Celada A, Lawrence T, Otsu K,

bioRxiv preprint doi: https://doi.org/10.1101/151852; this version posted June 19, 2017. The copyright holder for this preprint (which was not certified by peer review) is the author/funder, who has granted bioRxiv a license to display the preprint in perpetuity. It is made available under aCC-BY-NC-ND 4.0 International license.

Brissette JL, Arthur JSC, et al. (2008) The kinase p38 alpha serves cell type-specific inflammatory functions in skin injury and coordinates pro- and anti-inflammatory gene expression. *Nat Immunol* **9**: 1019–1027.

17. Staples CJ, Owens DM, Maier J V., Cato ACB, Keyse SM (2010) Cross-talk between the p38α and JNK MAPK pathways mediated by MAP kinase phosphatase-1 determines cellular sensitivity to UV radiation. *J Biol Chem* **285**: 25928–25940.

18. Fosbrink M, Aye-Han N-N, Cheong R, Levchenko A, Zhang J (2010) Visualization of JNK activity dynamics with a genetically encoded fluorescent biosensor. *Proc Natl Acad Sci U S A* **107**: 5459–5464.

19. Komatsu N, Aoki K, Yamada M, Yukinaga H, Fujita Y, Kamioka Y, Matsuda M (2011) Development of an optimized backbone of FRET biosensors for kinases and GTPases. *Mol Biol Cell* **22**: 4647–4656.

20. Tomida T, Takekawa M, Saito H (2015) Oscillation of p38 activity controls efficient pro-inflammatory gene expression. *Nat Commun* **6**: 8350.

21. Regot S, Hughey JJ, Bajar BT, Carrasco S, Covert MW (2014) High-sensitivity measurements of multiple kinase activities in live single cells. *Cell* **157**: 1724–1734.

22. Hao N, Budnik BA, Gunawardena J, O'Shea EK (2013) Tunable Signal Processing Through Modular Control of Transcription Factor Translocation. *Science (80-)* **339**: 460 LP-464.

23. Komeili A, O'Shea EK (1999) Roles of phosphorylation sites in regulating activity

bioRxiv preprint doi: https://doi.org/10.1101/151852; this version posted June 19, 2017. The copyright holder for this preprint (which was not certified by peer review) is the author/funder, who has granted bioRxiv a license to display the preprint in perpetuity. It is made available under aCC-BY-NC-ND 4.0 International license.

of the transcription factor Pho4. *Science (80-)* **284**: 977–980.

24. Nardozzi JD, Lott K, Cingolani G (2010) Phosphorylation meets nuclear import: a review. *Cell Commun Signal* **8**: 32.

25. Obsil T, Obsilova V (2008) Structure/function relationships underlying regulation of FOXO transcription factors. *Oncogene* **27**: 2263–2275.

26. Engel K, Kotlyarov A, Gaestel M (1998) Leptomycin B-sensitive nuclear export of MAPKAP kinase 2 is regulated by phosphorylation. *EMBO J* **17**: 3363–3371.

27. Meng W, Swenson LL, Fitzgibbon MJ, Hayakawa K, Haar E Ter, Behrens AE, Fulghum JR, Lippke J a. (2002) Structure of mitogen-activated protein kinase-activated protein (MAPKAP) kinase 2 suggests a bifunctional switch that couples kinase activation with nuclear export. *J Biol Chem* **277**: 37401–37405.

28. Trask OJ, Baker A, Williams RG, Nickischer D, Kandasamy R, Laethem C, Johnston PA, Johnston PA (2006) Assay Development and Case History of a 32K-Biased Library High-Content MK2-EGFP Translocation Screen to Identify p38 Mitogen-Activated Protein Kinase Inhibitors on the ArrayScan 3.1 Imaging Platform. *Methods Enzymol* **414**: 419–439.

29. Kim JH, Lee SR, Li LH, Park HJ, Park JH, Lee KY, Kim MK, Shin BA, Choi SY (2011) High cleavage efficiency of a 2A peptide derived from porcine teschovirus-1 in human cell lines, zebrafish and mice. *PLoS One* **6**: 1–8.

30. Pereira L, Igea A, Canovas B, Dolado I, Nebreda AR (2013) Inhibition of p38 MAPK sensitizes tumour cells to cisplatin-induced apoptosis mediated by reactive oxygen species and JNK. *EMBO Mol Med* **5**: 1759–1774.

bioRxiv preprint doi: https://doi.org/10.1101/151852; this version posted June 19, 2017. The copyright holder for this preprint (which was not certified by peer review) is the author/funder, who has granted bioRxiv a license to display the preprint in perpetuity. It is made available under aCC-BY-NC-ND 4.0 International license.

31. Arthur JSC, Ley SC (2013) Mitogen-activated protein kinases in innate immunity. *Nat Rev Immunol* **13**: 679–692.

32. Grollman AP (1967) Inhibitors of protein biosynthesis. II. Mode of action of anisomycin. *Biol Chem* **242**: 3226–3233.

33. Ferreiro I, Joaquin M, Islam A, Gomez-Lopez G, Barragan M, Lombardía L, Domínguez O, Pisano DG, Lopez-Bigas N, Nebreda AR, et al. (2010) Whole genome analysis of p38 SAPK-mediated gene expression upon stress. *BMC Genomics* **11**: 144.

34. Brock A, Chang H, Huang S (2009) Non-genetic heterogeneity--a mutation-independent driving force for the somatic evolution of tumours. *Nat Rev Genet* **10**: 336–342.

35. Wakamoto Y, Dhar N, Chait R, Schneider K, Signorino-Gelo F, Leibler S, McKinney JD, Chemistry T (2013) Dynamic Persistence of Antibiotic-Stressed Mycobacteria. *Science (80-)* **339**: 91–95.

36. Kawakami K, Noda T (2004) Transposition of the Tol2 Element, an Ac-Like Element from the Japanese Medaka Fish Oryzias latipes, in Mouse Embryonic Stem Cells. *Genetics* **166**: 895–899.

37. Niwa H, Yamamura K, Miyazaki J (1991) Efficient selection for high-expression transfectants with a novel eukaryotic vector. *Gene* **108**: 193–199.

38. Yusa K, Rad R, Takeda J, Bradley A (2009) Generation of transgene-free induced pluripotent mouse stem cells by the piggyBac transposon. *Nat Methods* **6**: 363–369.

bioRxiv preprint doi: https://doi.org/10.1101/151852; this version posted June 19, 2017. The copyright holder for this preprint (which was not certified by peer review) is the author/funder, who has granted bioRxiv a license to display the preprint in perpetuity. It is made available under aCC-BY-NC-ND 4.0 International license.

39. Sanjana NE, Shalem O, Zhang F (2014) Improved vectors and genome-wide libraries for CRISPR screening. *Nat Methods* **11**: 783–784.

40. Maryu G, Matsuda M, Aoki K (2016) Multiplexed fluorescence imaging of ERK and Akt activities and cell-cycle progression. *Cell Struct Funct* **92**: 81–92.

Figure legends

Figure 1 - Establishment of a multiplexed imaging system for monitoring JNK and p38 kinase activities with high specificity and sensitivity.

A Schematic of the phosphorylation-mediated translocation of a kinase translocation reporter (KTR).

B HeLa cells stably expressing p38 KTR-mEGFP and mEGFP-MK2, respectively, were stimulated with 1 μg/ml anisomycin. Representative images before and after 20 min of anisomycin stimulation and averaged C/N ratios are shown. Scale bar: 20 μm. n = 38 cells for p38 KTR-mEGFP, n = 34 cells for mEGFP-MK2 from two independent experiments.

C Structure and representative images of the JNK reporter JNK KTR-mCherry, p38 reporter mKO-MK2, and nuclear marker NLS-iRFP-NLS. NLS, nuclear localization signal; NES, nuclear export signal; P, phosphorylation sites. Scale bar: 20 μm.

D Clonal HeLa cells stably expressing JNK KTR-mCherry, mKO-MK2, and NLS-iRFP-NLS were stimulated with 1 μg/ml anisomycin and imaged over time. Scale bar: 20 μm.

E C/N ratios of JNK KTR-mCherry and mKO-MK2 were quantified for single cells after 1 μg/ml anisomycin stimulation. n = 20 cells each.

F Cells were stimulated with 1 μg/ml anisomycin and treated with 10 μM JNK inhibitor VIII (JNKiVIII), 10 μM of the p38 inhibitor SB203580 (SB), or 0.1% DMSO at the indicated time point (arrow). Averaged JNK KTR-mCherry and mKO-MK2 C/N ratios are shown. n = 20 cells for each condition.

G HeLa wildtype, *MAPK8/9* (*JNK1/2*) double KO, and *MAPK14* (*p38α*) KO cells stably expressing the poly-cistronic reporter construct NJP, which encodes NLS-iRFP-NLS, JNK KTR-mCherry, and mKO-MK2, connected by self-cleaving P2A peptides,

bioRxiv preprint doi: https://doi.org/10.1101/151852; this version posted June 19, 2017. The copyright holder for this preprint (which was not certified by peer review) is the author/funder, who has granted bioRxiv a license to display the preprint in perpetuity. It is made available under aCC-BY-NC-ND 4.0 International license.

were stimulated with 1 μg/ml anisomycin. Averaged JNK KTR-mCherry and mKO-MK2 C/N ratios are shown. n = 20 cells for each condition.

H The time courses of the normalized p-JNK/JNK and p-p38/p38 ratios upon 1 μg/ml anisomycin stimulation were compared with the normalized mKO-MK2 and JNK KTR-mCherry C/N ratios, respectively. n = 3 for western blot data, n = 20 cells for imaging data.

I Dose-response curves of the JNK KTR-mCherry and mKO-MK2 C/N ratios after 1 h of anisomycin stimulation are shown. Experimental data were fitted with the Hill function and derived EC50 values and Hill coefficients (nH) are indicated. n ≥ 100 cells for each condition, from at least three independent experiments.

J JNK KTR-mCherry C/N and mKO-MK2 C/N ratios linearly correlate with normalized p-JNK/JNK and p-p38/p38 ratios, respectively. Imaging and western blot data were obtained after 1 h of treatment with various doses of anisomycin and/or SB203580. Scatterplots were fitted to a linear regression and the obtained Pearson correlation values are shown. n = 3 for western blot data and n ≥ 60 cells for imaging data.

Data information: In (B, F-J), data are presented as the mean with SD.

Figure 2 - Cross-inhibition of JNK activity by p38 under various stress conditions.

A Clonal HeLa cells stably expressing JNK KTR-mCherry, mKO-MK2, and NLS-iRFP-NLS were pretreated with 0.1% DMSO and 10 μM SB203580, respectively, and then stimulated with 10 ng/ml TNFα, 10 ng/ml IL-1β, 10 ng/ml anisomycin, 200 mM sorbitol, 100 J/m^2 UV-C, or imaging medium as control. Representative images of JNK KTR-mCherry and mKO-MK2 after 30 min of treatment with TNFα and 1 h of treatment with the other stimuli are shown.

B Clonal HeLa cells stably expressing JNK KTR-mCherry, mKO-MK2, and NLS-iRFP-NLS were pretreated with 0.1% DMSO, 10 μM SB203580, or 1 μM VX-745, and then stimulated with 10 ng/ml TNFα, 10 ng/ml IL-1β, 10 ng/ml anisomycin, 200 mM sorbitol, or 100 J/m^2 UV-C, and imaged over time. Averaged JNK KTR-mCherry and mKO-MK2 C/N ratios are shown. n = 50 cells for each condition from two independent experiments.

bioRxiv preprint doi: https://doi.org/10.1101/151852; this version posted June 19, 2017. The copyright holder for this preprint (which was not certified by peer review) is the author/funder, who has granted bioRxiv a license to display the preprint in perpetuity. It is made available under aCC-BY-NC-ND 4.0 International license.

C JNK KTR-mCherry and mKO-MK2 C/N ratios are displayed as heat maps for cells from (B). Each line of the JNK KTR-mCherry and mKO-MK2 C/N ratios represents the activity dynamics in a single cell, with red colors indicating high and blue colors indicating low kinase activities. n = 50 cells for each condition from two independent experiments.

D Clonal HeLa cells stably expressing JNK KTR-mCherry, mKO-MK2, and NLS-iRFP-NLS were pretreated with the indicated concentrations of SB203580 and stimulated with 10 ng/ml anisomycin for 1 h. Averaged JNK KTR-mCherry C/N ratios are plotted against averaged mKO-MK2 C/N ratios for each condition and fitted to a linear regression model. The Pearson correlation coefficient R is indicated. n = 20 cells for each condition.

E Clonal HeLa cells stably expressing JNK KTR-mCherry, mKO-MK2, and NLS-iRFP-NLS were pretreated with 0.1% DMSO or 10 μM SB203580 and stimulated with various doses of anisomycin. JNK KTR-mCherry C/N ratios at 60 min of treatment were averaged. The dose responses were fitted with the Hill function (black lines). EC50 values and Hill coefficients (nH) are indicated. n ≥ 86 cells per condition from two independent experiments.

F Distributions of JNK KTR-mCherry C/N ratios at 60 min of anisomycin treatment for 0.1% DMSO and 10 μM SB203580 -pretreated reporter cells. n ≥ 86 cells per condition from two independent experiments.

G HeLa cells were pretreated with 0.1% DMSO (D) or 10 μM SB203580 (SB) and then stimulated with 10 ng/ml TNFα for 30 min, 10 ng/ml IL-1β for 60 min, 10 ng/ml anisomycin for 60 min, 200 mM sorbitol for 60 min, or 100 J/m2 UV-C for 60 min. Cell lysates were analyzed by western blotting against p-p38, p38, p-JNK, and JNK. Representative blots out of three independent experiments are shown. The SB/DMSO ratio is calculated as the fold change of the p-p38/p38 or p-JNK/JNK in the SB203580 over DMSO control treated samples. n=3 for each condition.

Data information: In (B, D, and E), data are presented as the mean with SD. In (G), significance was tested by a Student's *t*-test. ns = not significant, * $p<0.05$.

Figure 3 - Transcriptional and post-translational mechanisms contribute to

bioRxiv preprint doi: https://doi.org/10.1101/151852; this version posted June 19, 2017. The copyright holder for this preprint (which was not certified by peer review) is the author/funder, who has granted bioRxiv a license to display the preprint in perpetuity. It is made available under aCC-BY-NC-ND 4.0 International license.

repression of JNK activity by p38.

A Clonal HeLa cells stably expressing JNK KTR-mCherry, mKO-MK2, and NLS-iRFP-NLS were pretreated with 0.1% DMSO, 1 μg/ml actinomycin D, or 10 μM SB203580, then stimulated with 10 ng/ml TNFα, 10 ng/ml IL-1β, 10 ng/ml anisomycin, 200 mM sorbitol, or 100 J/m^2 UV-C, and imaged over time. Averaged JNK KTR-mCherry and mKO-MK2 C/N ratios are shown. n = 70 cells per condition from at least two independent experiments.

B Normalized JNK and p38 activation and post-translational and transcriptional cross-inhibition of JNK by p38 are indicated for 200 mM sorbitol at 120 min, 10 ng/ml TNFα at 30 min, 10 ng/ml IL-1β at 42 min, 100 J/m^2 UV-C at 120 min, and 10 ng/ml anisomycin stimulation at 120 min. The relative contribution of post-translational and transcriptional cross-inhibition differs for the various stimuli. Data from (A) were normalized by minimum and maximum values from Fig 1J.

C Clonal HeLa cells stably expressing JNK KTR-mCherry, mKO-MK2, and NLS-iRFP-NLS were pretreated with 0.1% DMSO, 1 μg/ml actinomycin D, or 10 μM SB203580 and stimulated with various doses of IL-1β. Since the time of the peak activity shifted, the maximal JNK KTR-mCherry and mKO-MK2 C/N ratios within 60 min after stimulation were selected and averaged. The dose responses were fitted with the Hill function (black lines). EC50 values and Hill coefficients (nH) are indicated. n = 60 cells per condition from two independent experiments.

Data information: In (A and C), data are presented as the mean with SD.

Figure 4 - TAB1 phosphorylation mediates post-translational cross-inhibition upon cytokine stimulation.

A HeLa wildtype, *TAB1* KO, and *TAK1* KO cells, stably expressing the polycistronic construct NJP were stimulated with 10 ng/ml TNFα for 30 min, 10 ng/ml IL-1β for 50 min, 10 ng/ml anisomycin for 60 min, or 200 mM sorbitol for 20 min, or were exposed to 100 J/m^2 UV-C and observed after 20 min. Averaged JNK KTR-mCherry C/N ratios are shown. Dashed lines indicate basal C/N ratios. n ≥ 34 cells for each condition from at least two independent experiments. Significance was tested against the wildtype control.

bioRxiv preprint doi: https://doi.org/10.1101/151852; this version posted June 19, 2017. The copyright holder for this preprint (which was not certified by peer review) is the author/funder, who has granted bioRxiv a license to display the preprint in perpetuity. It is made available under aCC-BY-NC-ND 4.0 International license.

B Averaged mKO-MK2 C/N ratios are shown for the same cells and conditions from (A). Dashed lines indicate basal C/N ratios. n ≥ 34 cells for each condition from at least two independent experiments.

C HeLa wildtype, *TAB1* KO, and *TAB1* KO cells either complemented with TAB1 wildtype or TAB1 S423A T431A (SATA), stably expressing NJP were stimulated with 10 ng/ml TNFα for 30 min, 10 ng/ml IL-1β for 50 min, or 200 mM sorbitol for 20 min. Averaged JNK KTR-mCherry and mKO-MK2 C/N ratios are shown. Dashed lines indicate basal C/N ratios. n ≥ 37 cells from at least two independent experiments.

D Schematic of post-translational cross-inhibition of JNK by p38. The TAK1/TAB1 complex might mediate cross-inhibition of JNK by p38, when stimulated with the cytokines TNFα and IL-1β. Other upstream kinases are probably involved in the JNK repression under other stress conditions.

Data information: In (A - C), data are presented as the mean with SD. Significance in (A - C) was tested by a Student's *t*-test. ns, not significant; *p<0.05, **p<0.01, ***p<0.001.

Figure 5 - Cross-inhibition by p38 causes cell-to-cell variability of stress and cytokine-induced JNK activities.

A Histograms of the JNK KTR-mCherry and mKO-MK2 C/N ratio distribution in 0.1% DMSO or 10 μM SB203580 -pretreated cells at 60 min of 10 ng/ml anisomycin stimulation. The coefficient of variation (CV) is indicated. n ≥ 350 cells per condition from four independent experiments.

B The time course of the coefficient of variation (CV) upon 10 ng/ml anisomycin stimulation is shown for the JNK KTR-mCherry and mKO-MK2 C/N ratios in 0.1% DMSO or 10 μM SB203580 -pretreated cells. n = 50 cells per condition from two independent experiments.

C The coefficients of variation of the JNK KTR-mCherry and mKO-MK2 C/N ratios at 30 min of 10 ng/ml TNFα, 60 min of 10 ng/ml IL-1β, 60 min of 10 ng/ml anisomycin, 60 min of 200 mM sorbitol, or 60 min of 100 J/m^2 UV-C treatment are shown for 0.1% DMSO or 10 μM SB203580 -pretreated clonal reporter cells. n = 50 cells per condition from two independent experiments.

bioRxiv preprint doi: https://doi.org/10.1101/151852; this version posted June 19, 2017. The copyright holder for this preprint (which was not certified by peer review) is the author/funder, who has granted bioRxiv a license to display the preprint in perpetuity. It is made available under aCC-BY-NC-ND 4.0 International license.

D p38 antagonizes JNK by post-translational and transcriptional mechanisms upon cytokine and stress stimulation. The relative contribution of the two modes of cross-inhibition depends on the type of agonist. This cross-inhibition of JNK might induce cell-to-cell variability in JNK activity, while p38 activity is more uniform among cells.

Data information: In (A-C), the coefficient of variation is given as the SD/mean.

Expanded View Figure legends

Figure EV1 - Characterization of a multiplexed imaging system for monitoring JNK and p38 kinase activities.

A The fold increases in the C/N ratios of p38 KTR-mEGFP and mEGFP-MK2 after 30 min of 1 μg/ml anisomycin stimulation are shown for single cells and as an average (red line). n ≥ 50 cells for each condition from two independent experiments.

B Bleed-through analysis of JNK KTR-mCherry, mKO-MK2, and NLS-iRFP-NLS. HeLa cells stably expressing single reporters were imaged in each fluorescent channel and images are represented in a pseudo-color scale. The values shown represent the fraction of fluorescence leakage. Scale bar: 60 μm.

C Plasmid structure of the polycistronic pNJP reporter construct, consisting of NLS-iRFP-NLS, JNK KTR-mCherry, and mKO-MK2, connected by self-cleaving P2A peptide sequences, so that the reporters are expressed separately. The P2A peptide sequence and point of cleavage (red arrowhead) are indicated.

D Representative images of NLS-iRFP-NLS, JNK KTR-mCherry, and mKO-MK2, stably expressed from NJP in HeLa cells. Scale bars: 20 μm.

E HeLa control cells and cells stably expressing JNK KTR-mCherrry, mKO-MK2 or the polycistronic construct NJP were lysed and analyzed by western blotting against mCherry and mKO. JNK KTR-mCherry (33.6 kDa) and mKO-MK2 (70.2 kDa) samples served as a positive control (red arrowhead).

F JNK KTR-mCherry and mKO-MK2 were transiently overexpressed (left) or stably expressed by transposon-mediated gene-transfer, i.e., the PiggyBac transposon system (right) in HeLa cells and stimulated with 1 μg/ml anisomycin for 1 h. The JNK KTR-mCherry and mKO-MK2 C/N ratios of single cells were plotted against basal nuclear mCherry and mKO intensities, respectively, on a logarithmic scale. The scatterplots

bioRxiv preprint doi: https://doi.org/10.1101/151852; this version posted June 19, 2017. The copyright holder for this preprint (which was not certified by peer review) is the author/funder, who has granted bioRxiv a license to display the preprint in perpetuity. It is made available under aCC-BY-NC-ND 4.0 International license.

were fitted to a linear regression and the obtained Pearson correlation values are shown. n ≥ 40 cells for each condition.

G KO of *MAPK14* (*p38α*) and double KO of *MAPK8* (*JNK1*) and *MAPK9* (JNK2) were confirmed by western blotting against total p38, JNK1, JNK2, and α-tubulin as a control.

H HeLa cells were treated with 1 μg/ml anisomycin for the indicated times. Cell lysates were analyzed by western blotting against p-p38, total p38, p-JNK, and total JNK. Representative blots out of three independent experiments are shown.

I Clonal HeLa cells stably expressing JNK KTR-mCherry, mKO-MK2, and NLS-iRFP-NLS were titrated with anisomycin and imaged 1 h after stimulation. Representative images are shown.

J HeLa cells were treated with the indicated doses of anisomycin for 1 h. Cell lysates were analyzed by western blotting against p-p38, total p38, p-JNK, and total JNK. Representative blots out of three independent experiments are shown.

Data information: In (A and F) single cell data are shown. Significance in (A) was tested by a Student's *t*-test. ***p<0.001.

Figure EV2 - Crosstalk of JNK and p38 kinase.

A Clonal HeLa cells stably expressing JNK KTR-mCherry, mKO-MK2, and NLS-iRFP-NLS pretreated with the indicated doses of SB203580, then stimulated with 10 ng/ml anisomycin, and imaged over time. Averaged JNK KTR-mCherry and mKO-MK2 C/N ratios are shown. n = 20 cells for each condition.

B Clonal HeLa cells stably expressing JNK KTR-mCherry, mKO-MK2, and NLS-iRFP-NLS were pretreated with 0.1% DMSO or 10 μM JNK inhibitor VIII, then stimulated with 10 ng/ml TNFα, 10 ng/ml IL-1β, 10 ng/ml anisomycin, 200 mM sorbitol, or 100 J/m^2 UV-C, and imaged over time. Averaged JNK KTR-mCherry and mKO-MK2 C/N ratios are shown. n = 50 cells for each condition from two independent experiments.

Data information: In (A), data are represented as the mean. In (B), data are represented as the mean with SD.

bioRxiv preprint doi: https://doi.org/10.1101/151852; this version posted June 19, 2017. The copyright holder for this preprint (which was not certified by peer review) is the author/funder, who has granted bioRxiv a license to display the preprint in perpetuity. It is made available under aCC-BY-NC-ND 4.0 International license.

Figure EV3 - p38 cross-inhibits JNK by transcriptional and post-translational mechanisms.

Clonal HeLa cells stably expressing JNK KTR-mCherry, mKO-MK2, and NLS-iRFP-NLS were pretreated with 0.1% DMSO, 10 µM SB203580, and 1 µg/ml actinomycin D, respectively, and then stimulated with 10 ng/ml TNFα, 10 ng/ml IL-1β, 10 ng/ml anisomycin, 200 mM sorbitol, or 100 J/m^2 UV-C. The JNK KTR-mCherry and mKO-MK2 C/N ratios are represented for single cells in heat maps. Each tandem arranged line of JNK KTR-mCherry and mKO-MK2 C/N ratios represents the activity dynamics in a single cell, with red colors indicating high and blue colors indicating low kinase activities. n = 70 cells for each condition from at least two independent experiments.

Figure EV4 - The role TAB1/TAK1 in post-translational JNK cross-inhibition

A Western blot analysis of the expression levels of TAB1 in wildtype (wt) cells, clonal *TAB1* KO cells, *TAB1* KO cells stably expressing an empty control construct, *TAB1* KO cells rescued by stable expression of TAB1-wt, and *TAB1* KO cells stably expressing TAB1 S423A T431A (SATA). α-Tubulin was used as a loading control.

B Western blot analysis of the expression levels of TAK1 in the wildtype (wt) and *MAP3K7* KO cells. α-Tubulin was used as a loading control.

C mEGFP-TAK1, Flag-TAB1-wt, SATA, and S423E T431E (SETE) were transiently expressed in HeLa cells, when indicated. Total lysates and immunoprecipitated samples with an anti-GFP antibody were subjected to western blot analysis with anti-GFP, anti-TAK1 and anti-Flag.

Figure EV5 - Cell to cell variability of JNK and p38 activity upon inflammatory and stress stimuli

Clonal HeLa cells stably expressing JNK KTR-mCherry, mKO-MK2, and NLS-iRFP-NLS were pretreated with 0.1% DMSO or 10 µM SB203580, stimulated with 10 ng/ml TNFα, 10 ng/ml IL-1β, 10 ng/ml anisomycin, 200 mM sorbitol, or 100 J/m^2 UV-C, and imaged over time. The time course of the coefficient of variation (CV) is shown for the JNK KTR-mCherry and mKO-MK2 C/N ratios. n = 50 cells per condition from two independent experiments.

bioRxiv preprint doi: https://doi.org/10.1101/151852; this version posted June 19, 2017. The copyright holder for this preprint (which was not certified by peer review) is the author/funder, who has granted bioRxiv a license to display the preprint in perpetuity. It is made available under aCC-BY-NC-ND 4.0 International license.

Data information: The coefficient of variation is given as the SD/mean.

Expanded View Movie Legend

Movie EV1 – Multiplexed imaging system for monitoring JNK and p38 activities.

HeLa cells stably expressing JNK KTR-mCherry (top left), mKO-MK2 (top right), and NLS-iRFP-NLS (bottom left) were imaged every 2 min. 10 ng/ml anisomycin was added at elapsed time point 0 min. Scale bar: 50 μm.

bioRxiv preprint doi: https://doi.org/10.1101/151852; this version posted June 19, 2017. The copyright holder for this preprint (which was not certified by peer review) is the author/funder, who has granted bioRxiv a license to display the preprint in perpetuity. It is made available under aCC-BY-NC-ND 4.0 International license.

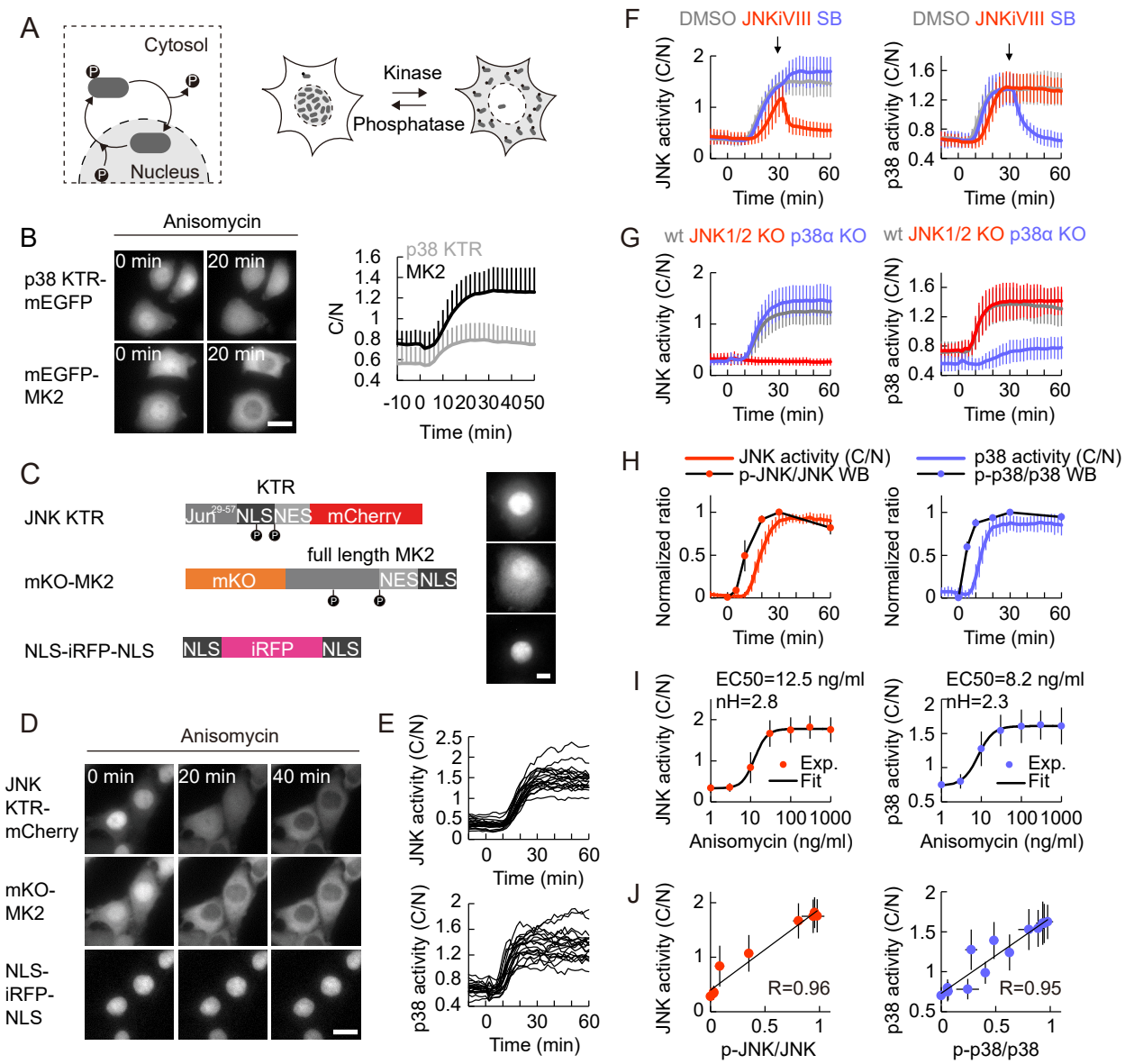

bioRxiv preprint doi: https://doi.org/10.1101/151852; this version posted June 19, 2017. The copyright holder for this preprint (which was not certified by peer review) is the author/funder, who has granted bioRxiv a license to display the preprint in perpetuity. It is made available under aCC-BY-NC-ND 4.0 International license.

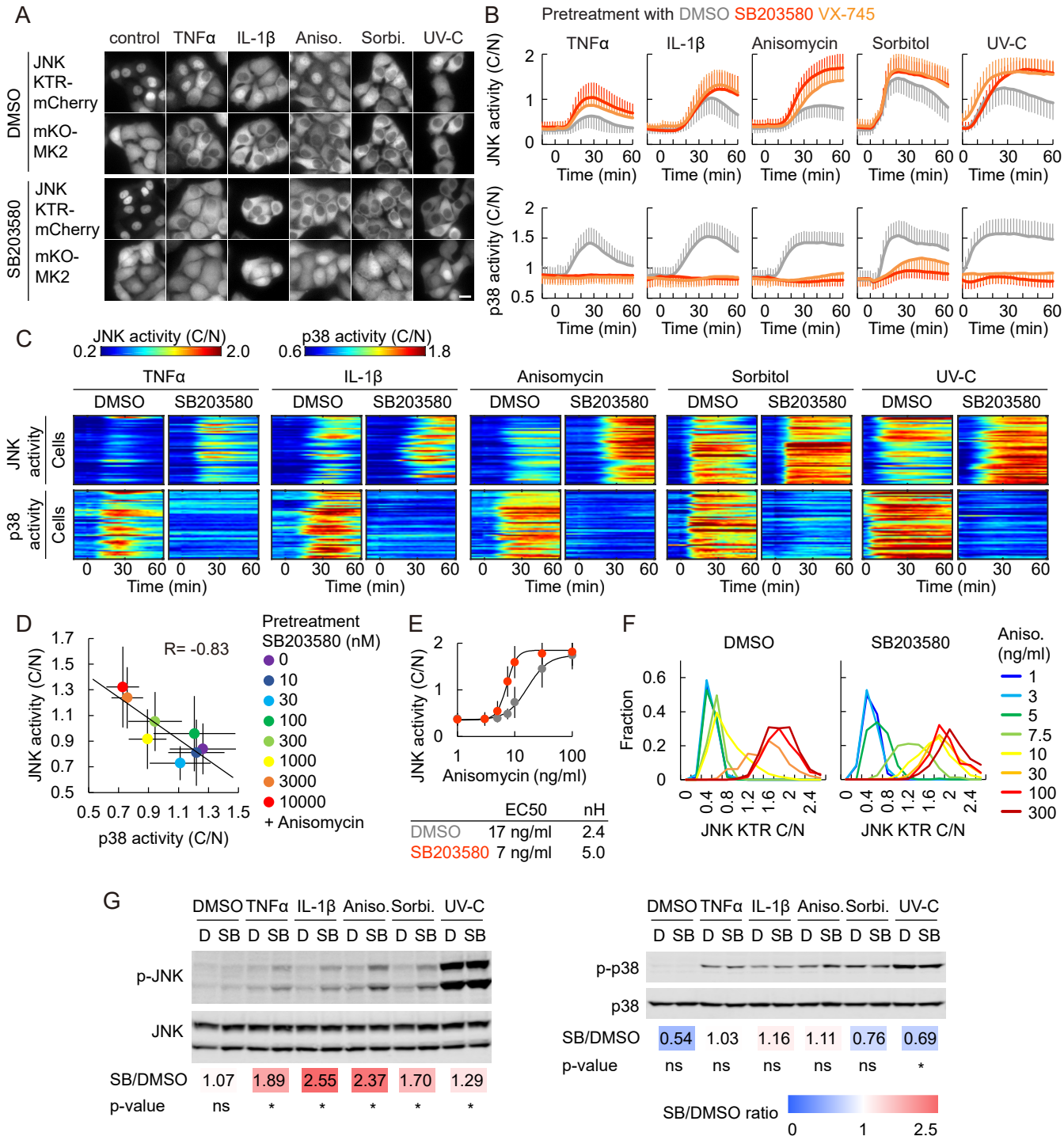

bioRxiv preprint doi: https://doi.org/10.1101/151852; this version posted June 19, 2017. The copyright holder for this preprint (which was not certified by peer review) is the author/funder, who has granted bioRxiv a license to display the preprint in perpetuity. It is made available under aCC-BY-NC-ND 4.0 International license.

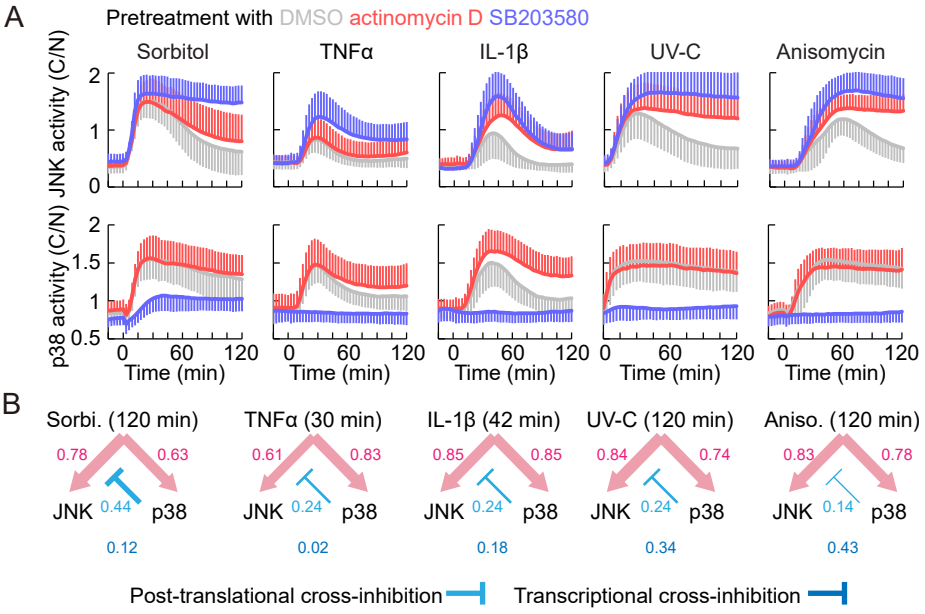

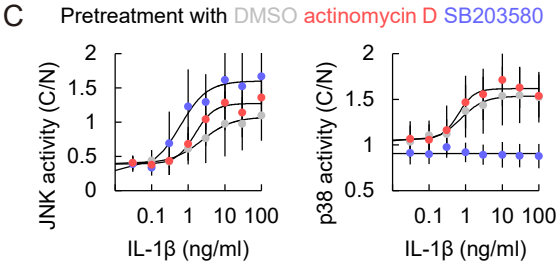

JNK activity	EC50	nH
DMSO	2.4 ng/ml	1.0
actinomycin D	1.5 ng/ml	1.7
SB203580	0.6 ng/ml	1.2

p38 activity	EC50	nH
DMSO	0.7 ng/ml	1.4
actinomycin D	0.6 ng/ml	2.0
SB203580	-	-

bioRxiv preprint doi: https://doi.org/10.1101/151852; this version posted June 19, 2017. The copyright holder for this preprint (which was not certified by peer review) is the author/funder, who has granted bioRxiv a license to display the preprint in perpetuity. It is made available under aCC-BY-NC-ND 4.0 International license.

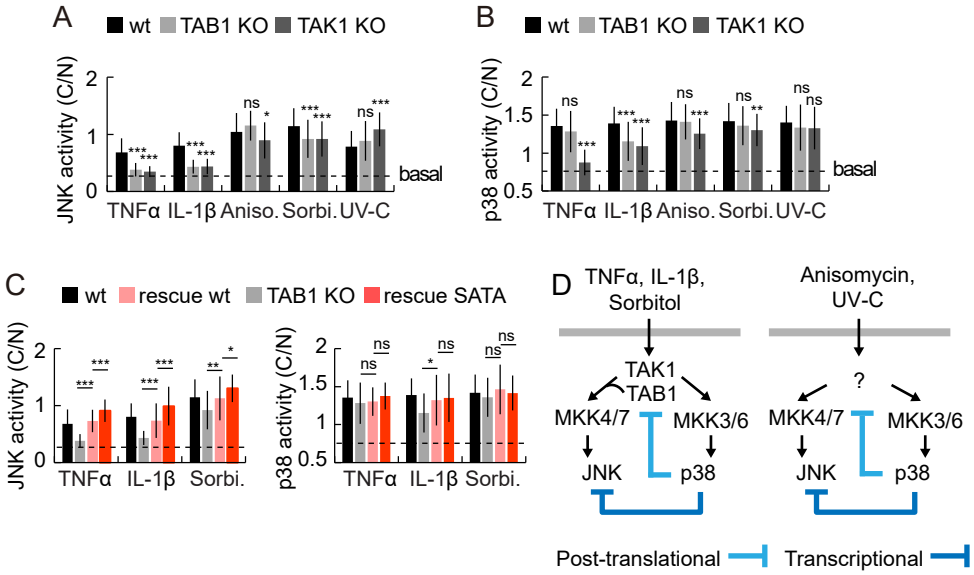
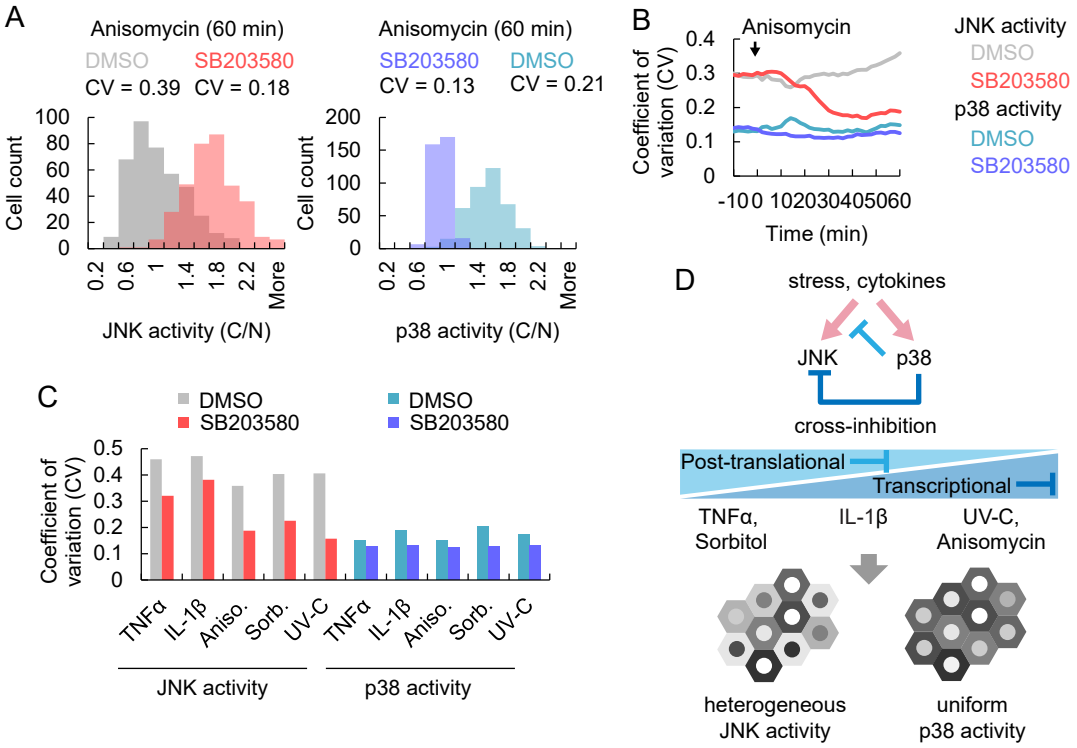
bioRxiv preprint doi: https://doi.org/10.1101/151852; this version posted June 19, 2017. The copyright holder for this preprint (which was not certified by peer review) is the author/funder, who has granted bioRxiv a license to display the preprint in perpetuity. It is made available under aCC-BY-NC-ND 4.0 International license.